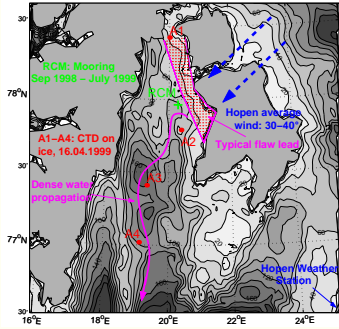


## 1 Winter Observations in Storfjorden

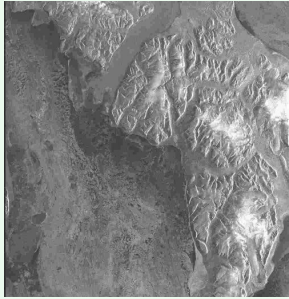


During the winter season 1998/99 we have performed helicopter field work in Storfjorden and obtained several CTD stations on thin ice. Our aim was to study the formation process of dense water in the shallow (50 m) north and track the density changes from the formation area through the basin to the sill. During the whole winter season a mooring RCM operated close to the expected formation area of densest waters.

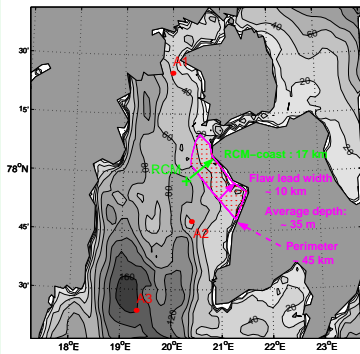
The RCM instrument was situated in a small channel through which the dense waters from the **flaw lead site** must drain to feed the basin. In April we were successful in obtaining four CTD profiles A1 - A4 on thin ice stations that can be linked to the mooring timeseries. We are interested in the initial density anomaly that formed in the North during strong meteorological forcing and ice growth in a flaw lead. Using the term **flaw lead site** in the following refers to either open water or thin ice.

## 3 The Flaw Lead Size

ERS2 SAR image 18.02.1999



ERS2 SAR image 21.02.1999



During another forcing event two ERS2 SAR images have been available. Preceding 18.02. winds have been offshore at 7-10 m/s and a flaw lead is seen as a dark signature. Preceding 21.02 the temperatures had been lower than -20°C, yet calm wind conditions let us interpret the bright signature as frost flowers on very thin ice. In both cases the flaw lead width is typically 10 km.

Looking at the bathymetry we suppose other constraints on the size of forcing area that feeds the drainage channel where the mooring RCM is located. These are the distance of 17 km of the RCM mooring from the coast and the shallowing towards the north, many shoals not visible on the map. This makes the observed flaw lead limit plausible.

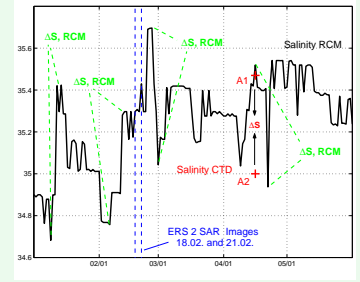
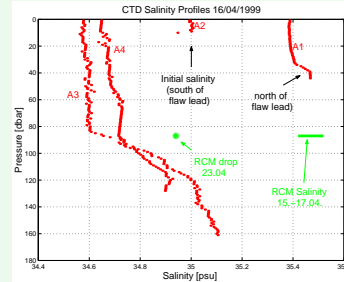
## 5 Scaling the Equilibrium Density Anomaly

The equilibrium density anomaly that may form in an area of isolated forcing is the density maximum that may be reached, before the baroclinic eddies along the rim of the region become so energetic that the eddy transport balances any further buoyancy increase. To compare our results to numerical predictions<sup>1-3</sup> we have to transform the scaling for a circular forcing region of radius  $r_0$  as follows.

$$\Delta b = g \frac{\Delta \rho}{\rho_0} = C \frac{(B_0 r_0)^{(2/3)}}{H} \text{ to } \Delta b = C \frac{(B_0 L_0)^{(2/3)}}{H}$$

with  $L_0$  being 2 times the polynya area per perimeter. Numerical predictions and laboratory studies cited in<sup>4</sup> give generally somewhat larger  $C$  between 6 and 9 than the theoretical prediction  $C=5$  from<sup>3</sup>. Field observations have not been published yet. To compute  $C$  for the four events we use an average  $B_0$  over 4 days from the peak preceding the salinity maxima.  $H$  and  $L_0$  are then computed by extending the forcing area towards the mooring and evaluating the average depth.

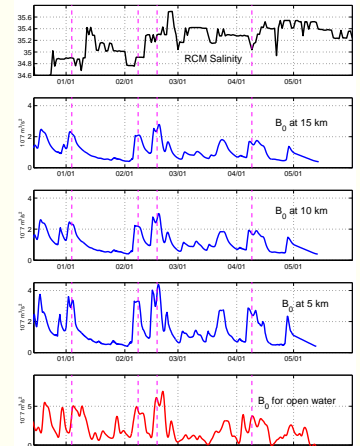
## 2 Comparison of Salinity Anomalies



The CTD observations from April are of particular value because they coincide with a maximum in the salinity time series. A closer look at the profiles and bathymetry shows that A2 should reasonably represent the source water south of the flaw lead. This station was obtained by landing on an iceberg that had grounded on a rather localized shoal. Station A1 in the North is then interpreted as the outcome of the preceding forcing event, having either formed locally under similar conditions or propagated northward. When comparing these observations with the mooring series we observe at the mooring intermittent drops to the upper layer salinity as measured at A2 are found. These large fluctuations agree in April both with maximum and initial salinities. From January to May we find four extreme events that may be interpreted in this way, they correspond to the strongest meteorological forcing events. These salinity differences taken from the timeseries will be interpreted as the maximum salinity increase that was created during a forcing event.

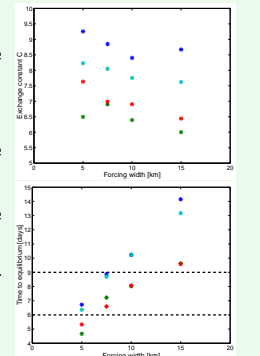
## 4 Computation of the Buoyancy Fluxes

A thin ice advection model has been run for the winter season to evaluate the buoyancy flux at different distances from the coast. The thermodynamic model largely follows Maykut's<sup>1</sup> formulation supplemented by brine rejection equations. Hopen winds are used to compute the one-dimensional advection along the western coastline. For comparison also the idealized open water fluxes are shown as an upper bound, yet the evaluation will be made simply for the reiterating thin ice growth and export budget that. The four major meteorological forcing events are indicated. These are leading the peaks in the salinity series by 6-9 days.



## 6 Results and Discussion

By implementing an ice model we arrive at values for  $C$  that are relatively independent of the chosen distance from coast. If we compare the time to reach equilibrium to the time lag between salinity and buoyancy flux (6-9 days) then 7.5 km seems to be the most probable average. Averaging the estimates for 5-10 km we find a best estimate of  $C=7.7 \pm 0.9$ . As the maximum possible buoyancy fluxes from open water exceed the effective thin ice buoyancy fluxes at these distances by a factor two, a lower bound for  $C$  assuming pure open water flaw leads would be about 5.



References: 1. Maykut, G. (1978): Energy exchange over young sea ice in the high Arctic. *J. Geophys. Res.*, 83, 3647-3658. 2. D.C. Chapman (1998): Setting the scales of the ocean response to isolated convection. *J. Oceanogr.*, 28, 606-620. 3. M.A. Spall and D. Chapman (1998): On the efficiency of baroclinic eddy heat transport across narrow fronts. *J. Oceanogr.*, 28, 2275-2286. 4. M. Visbeck, J. Marshall and H. Jones (1996): Dynamics of isolated convective regions in the ocean. *J. Oceanogr.*, 26, 1721-1734.